Available online at www.sciencedirect.com
SCIENCE DIRECT®
Journal of Power Sources 132 (2004) 309–314
JOURNAL OF POWER SOURCES
www.elsevier.com/locate/jpowsour

Short communication

Equivalent circuit parameters of nickel/metal hydride batteries from sparse impedance measurements

Sudarshan Rao Nelatury [a,*], Pritpal Singh [b]

[a] *SEET, 5091 Station Road, Penn State University Erie, Erie, PA 16563, USA*
[b] *Department of ECE, Villanova University, 800 Lancaster Ave., Villanova, PA 19085, USA*

Received 13 November 2003; accepted 12 December 2003

Abstract

In a recent communication, a method for extracting the equivalent circuit parameters of a lead acid battery from sparse (only three) impedance spectroscopy observations at three different frequencies was proposed. It was based on an equivalent circuit consisting of a bulk resistance, a reaction resistance and a constant phase element (CPE). Such a circuit is a very appropriate model of a lead-acid cell at high state of charge (SOC). This paper is a sequel to it and presents an application of it in case of nickel/metal hydride (Ni/MH) batteries, which also at high SOC are represented by the same circuit configuration. But when the SOC of a Ni/MH battery under interrogation goes low, The EIS curve has a positive slope at the low frequency end and our technique yields complex values for the otherwise real circuit parameters, suggesting the need for additional elements in the equivalent circuit and a definite relationship between parameter consistency and SOC. To improvise the previous algorithm, in order that it works reasonably well at both high and low SOCs, we propose three more measurements—two at very low frequencies to include the Warburg response and one at a high frequency to model the series inductance, in addition to the three in the mid frequency band—totally six measurements. In most of the today's instrumentation, it is the user who should choose the circuit configuration and the number of frequencies where impedance should be measured and the accompanying software performs data fitting by complex nonlinear least squares. The proposed method has built into it an SOC-based decision-making capability—both to choose the circuit configuration and to estimate the values of the circuit elements.

Keywords: Nickel/metal hydride batteries; Electrochemical impedance spectroscopy (EIS); Equivalent circuits

1. Introduction

We have witnessed a spate of research in the introduction of new electrochemical systems for memory backup applications. In our pursuit of high rate, high capacity batteries, Ni/MH batteries have emerged as efficient button cells, very useful for PCs and notebook computers. They are coming to the market in different sizes and shapes. Gauged with the results, they are promising, and research in the area of new generation Ni/MH technologies seems to be on the rise. Accordingly, the need to characterize these cells as accurately as possible, and estimate their SOC with least effort is a matter of immediate concern.

Ni/MH batteries are composed of a positive electrode made of nickel hydroxide, a negative electrode made of a hydrogen-absorbing alloy, a separator, alkaline electrolyte such as potassium hydroxide, a metal case and a sealing plate equipped with a safety valve. In the cylindrical type, the positive and negative electrodes are separated by the separator and coiled in a spiral inside the case, being sealed by the sealing plate through an insulation gasket. In the prismatic type, the positive and negative electrodes are separated by the separator and stacked in layers inside the case, being sealed by the sealing plate. The kinetic parameters of Ni/MH battery electrodes can be estimated from linear micro-polarization, Tafel polarization or by small signal electrochemical impedance spectroscopy (EIS) [1,2]. Also using EIS data, the charge/discharge mechanism of metal hydride electrode can be modeled [3–6]. In the rest of the paper, we discuss the equivalent circuit approach to interpret EIS data and explain how one might arrive at a more appropriate circuit model from sparse impedance measurements made at discrete frequencies. Our approach chooses the circuit model based on the calculated parameters and attempts to fit the EIS data to a reasonably good degree of accuracy.

* Corresponding author. Tel.: +1-814-898-6472; fax: +1-814-898-6125.
E-mail address: srn3@psu.edu (S.R. Nelatury).

0378-7753/$ – see front matter © 2004 Elsevier B.V. All rights reserved.
doi:10.1016/j.jpowsour.2003.12.013

2. Equivalent circuit modeling of Ni/MH battery

For an accurate model of any electrochemical device, one might employ a rigorous theory taking all the factors into consideration, but in practice that becomes too complicated. So, equivalent circuits may be used to relate the dynamical behavior of a battery. The small-signal behavior of an equivalent circuit model bears a correspondence with the terminal properties of the battery over a band of frequencies. Thus, arriving at a good model from the EIS data continues to be a challenge. The traditional approach in extracting these equivalent circuits is to collect as much EIS data as possible and subject it to complex nonlinear least squares algorithm. Champlin [7] identified the importance of sparse observations and proposed a technique involving measurement of real and imaginary parts of impedance of a cell at n (≥ 2) discrete frequencies to evaluate the component values of an equivalent circuit consisting of $2n$ circuit elements. The configuration chosen is a series RL circuit and few parallel RC sections all connected in series.

In a recent communication [8], we proposed a technique that elicits equivalent circuit parameters from sparse impedance data. The method relies on an equivalent circuit consisting of a bulk resistance, a reaction resistance and a constant phase element (CPE). The simplicity in the circuit topology chosen in [8] is justified by the principle of parsimony called "Occam's razor" highly favored in scientific philosophy. According to Boukamp [9], it is recommended that if the value of chi-square could decrease by 10-fold, introduction of a new circuit element is justified in the circuit model. In our experience with the Ni/MH cells, we found that the equivalent circuit used in [8] is good for cells with high SOC. But as SOC falls we find an upward bend shown in an oval in the Nyquist plot of Fig. 1 for 95% and 5% SOC.

It is known that at low SOC, the kinetics of the cell are greatly retarded and this can be modeled by a series Warburg impedance [10]. The Warburg response has a unit slope in the Nyquist plane. We might view it as a special case of CPE element whose impedance is of the form $1/D_{\mathrm{W}}(\mathrm{j}\omega)^{\psi_{\mathrm{W}}}$ with ψ_{W} close to 0.5. The Warburg response might not show up at high SOC as prominently as at low SOC, unless we measure at much lower frequencies. Thus, we need to modify the equivalent circuit by adding this extra element at low SOC.

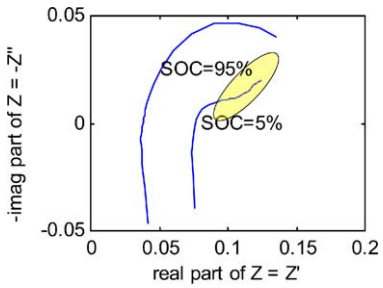

Fig. 1. Nyquist plot of EIS of a N/NH cell with 95 and 5% SOC.

This has to say that a proper choice of circuit configuration is also a task of determining SOC.

3. Choice of circuit configuration and extraction of parameters

To derive an electrical circuit using the sparse EIS data, we should have in mind what configuration or circuit topology we wish to use. For this purpose, we selected the two circuit configurations shown in Fig. 2a and b, circuit-2b being a superset of circuit-2a. The Warburg element is denoted by w in Fig. 2b.

As can be noted in Fig. 1, at the onset of the Warburg response we find an upward rise in the Nyquist plot. Let the Warburg impedance treated as a general CPE be expressed as

$$Z_{\mathrm{W}} = \frac{1}{D_{\mathrm{W}}(\mathrm{j}2\pi f)^{\psi_{\mathrm{W}}}} = Z''_{\mathrm{W}}(f) + \mathrm{j}Z''_{\mathrm{W}}(f) \tag{1}$$

Let $Z(f_{\mathrm{i}}) = Z'(f_{\mathrm{i}}) + \mathrm{j}Z''(f_{\mathrm{i}})$ denote the measured impedance at frequency f_{i}, with Z' and Z'' to represent real and imaginary parts respectively. At two low frequencies f_{L1} and f_{L2}, we wish to consider the slope of the curve

$$m = \frac{Z''(f_{\mathrm{L1}}) - Z''(f_{\mathrm{L2}})}{Z'(f_{\mathrm{L2}}) - Z'(f_{\mathrm{L1}})} \tag{2}$$

It is proposed to use circuit (b) if $m > 0$, and circuit (a) if $\mathrm{m} \leq 0$. If $\mathrm{m} > 0$ prevails, we shall propose the following trivial relations to get the Warburg values as:

$$\psi_{\mathrm{W}} = \frac{2}{\pi}\arctan(m) \tag{3}$$

$$D_{\mathrm{W}} = -\frac{\sin(\pi\psi_{\mathrm{W}}/2)}{2\pi f_{\mathrm{L2}} Z''(f_{\mathrm{L2}})\psi_{\mathrm{W}}} \tag{4}$$

We shall also select three mid frequencies f_{M1}, f_{M2}, f_{M3} ($f_{\mathrm{M3}}, > f_{\mathrm{M2}}, > f_{\mathrm{M1}}$), and extract values of R_{R}, CPE and R_{inf} using the algorithm presented in [8].

To estimate L, as we suggested in [8], we need a high frequency measurement at f_{H}. Ignoring the real part of the

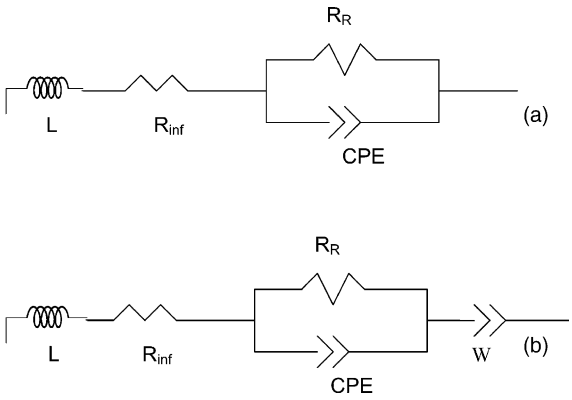

Fig. 2. Two circuit configurations chosen to fit EIS data for: (a) high SOC and (b) low SOC.

impedance at the far-end high frequency f_H, we write the following approximate expression for L as:

$$L = \frac{Z''(f_H)}{2\pi f_H} \tag{5}$$

Thus, Eqs. (2)–(5) permit extraction of the additional circuit elements in addition to the ones in [8]. At low-end of frequencies, we find that the negative reactance of the Warburg impedance dominates that of R_R–CPE section. Let us denote the impedance offered by L, R_{inf}, R_R and the CPE as:

$$Z_{ZARC}(f) = j2\pi fL + R_{inf} + \frac{R_R}{1 + R_R A_o (j\omega)^{\psi_{ZC}}} = Z'_{ZARC}(f) + jZ''_{ZARC}(f) \tag{6}$$

Then, if we are to interpolate the impedance at all the other frequencies based on the parameters of the circuit in Fig. 2a,

$$Z_{int}(f) = Z_{ZARC}(f) \tag{7}$$

But if the algorithm picks the circuit in Fig. 2b (which happens if m > 0), indicating medium or low SOC, we suggest the following interpolation formula:

$$Z_{int}(f) = Z''_{int}(f) + jZ''_{int}(f) \tag{8}$$

where

$$Z'_{int}(f) = Z'_{ZARC}(f) \tag{9}$$

for all f,

$$Z''_{int}(f) = \begin{cases} Z''_{ZARC}(f), & \text{if } Z''_{ZARC}(f) < Z''_W(f) \\ Z''_W(f), & \text{if } Z''_{ZARC}(f) \geq Z''_W(f) \end{cases} \tag{10}$$

for $f \leq f_{M3}$,

$$Z''_{int}(f) = Z''_{ZARC}(f) \tag{11}$$

for $f > f_{M3}$.

Thus, an algorithm like the above has a built-in decision making ability to rely on the Warburg reactance for low SOC at low frequencies and on the CPE element at mid frequencies and on the series inductance at far-end high frequency by the "brute-force" rule based knowledge acquisition and has the potential to emerge as a robust technique.

4. Simulation examples

In this paper, we took the EIS measurements on a Ni/MH battery at four different SOCs, viz., 95, 65, 35 and 5% and at 21 discrete frequencies in the range 1 Hz–100 kHz using Solartron SI 1280b and the accompanying ZPlot and ZView software for finding the equivalent circuit parameters. For purposes of comparison, we first considered fitting the entire 21 point EIS data with the choice of two circuits shown in Fig. 3a and b using these software utilities. These circuits gave better fit compared to other options. The bulk series resistance is represented by R_s. The circuit in Fig. 3a primarily attempts to fit the data by two time constants shown

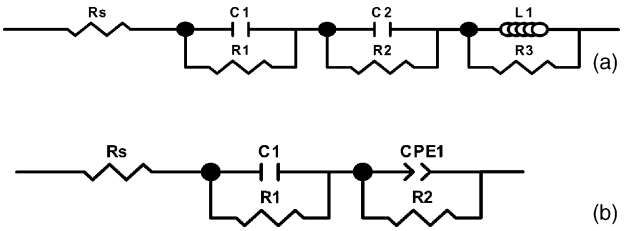

Fig. 3. Two circuit configurations chosen to fit EIS data using Solartron SI 1280B over the frequency band 1–10,000 Hz at discrete 21 frequencies.

by the RC sections, and since the impedance is dominated by inductance at the high frequency end, we also include an RL section. Fig. 3b does not have this inductance but it has a series resistance, one RC section and a Z_{ZARC} impedance involving a constant phase element.

Next the experiment is repeated with the method outlined in the present paper using the six frequencies {1, 1.58, 15.85, 63.1, 251.2, 10,000} Hz. Table 1 furnishes the circuit element values and a statistical comparison of all the models is made in Table 2. In particular, we computed three somewhat equivalent statistics: (a) correlation coefficient ρ between the measured and interpolated impedance, (b) error norm ||E||, which is just the Euclidian norm of the error, and (c) percent relative error defined as $e\% = 100||E||/||x||$, where x stands for measured real and imaginary parts of impedance appended as a data vector. From Table 1c, we find that when

Table 1
Values of the elements for the circuit in: (a) Fig. 3a, (b) Fig. 3b, and (c) using Eqs. (2)–(5) and circuits 2a and 2b

	SOC			
	95%	65%	35%	5%
(a) Circuit 3a				
R_s	0.038328	0.037838	0.042862	0.075998
C_1	0.7903	2.711	3.564	2.057
R_1	0.087744	0.030237	0.025531	0.032995
C_2	0.40835	0.26479	0.19985	0.045788
R_2	0.02892	0.023984	0.018568	0.023937
L_1	7.5939E−7	7.2315E−7	7.4886E−7	6.0951E−7
R_3	1.174E+13	1.174E+13	1.3949E+7	1.174E+13
(b) Circuit 3b				
R_s	0.038201	0.033976	0.035918	0.074651
C_1	12.35	0.80907	0.90384	0.20763
R_1	0.046716	0.013266	0.006833	0.008916
A_o	0.63602	8.175	16.9	12.99
ψ_{ZC}	0.85116	0.41125	0.24605	0.28644
R_2	0.10966	0.10379	2.596E+11	2.596E11
(c) Present method				
Slope m	−0.3304	0.2164	0.5111	0.4117
Circuit chosen	2a	2b	2b	2b
R_{inf}	0.038	0.0371	0.0421	0.0667
R_R	0.1249	0.0447	0.0343	0.0786
A_o	0.6745	0.8943	1.2891	2.8178
ψ_{ZC}	0.8357	0.769	0.6828	0.3569
L_1	7.4311E−7	7.1165E−7	7.4437E−7	6.2826E−7
D_W		9.8139	17.8276	11.9451
ψ_W		0.1357	0.3008	0.2486

Table 2
(a) Correlation coefficient, (b) error norm, and (c) percent relative error for the circuits 3a, 3b, and 2a + 2b combination at various SOCs.

	SOC			
	95%	65%	35%	5%
(a) Correlation coefficient				
Circuit 3a	0.9991	0.9989	0.9989	0.9989
Circuit 3b	0.9787	0.9589	0.9536	0.9886
Present method	0.9994	0.9983	0.9994	0.997
(b) Error norm				
Circuit 3a	0.9991	0.9989	0.9989	0.9989
Circuit 3b	0.9787	0.9589	0.9536	0.9886
Proposed method	0.9994	0.0119	0.0069	0.0088
(c) Percent relative rms error				
Circuit 3a	3.75	3.75	3.52	3.71
Circuit 3b	19.2	24.54	24.99	12.07
Proposed method	3.04	4.7974	2.6683	2.003

SOC is 95%, the algorithm has picked the configuration of circuit 2a yielding lesser e% and better ρ. And for SOC of 5%, circuit 2b is selected by the algorithm giving the least e% of 2.003%.

Also in a series of figures Figs. 4–10, we provide the EIS data measured and interpolated both in the complex Nyquist plane (a), as well as real and imaginary parts separately in (b) and (c) in each. The $y = x$ line in Figs. (b) and (c) shows ideal case when the interpolated and observed values coincide. In Fig. 7, we find the interpolated EIS based on circuit 3a deviating from the measured data at low frequencies with a downward trend (shown by an arrow) running repugnant to the idea of passive Warburg response at low SOC, disfavoring the use of discrete RC sections in stead of circuit elements CPE or W that exemplify a continuous distribution

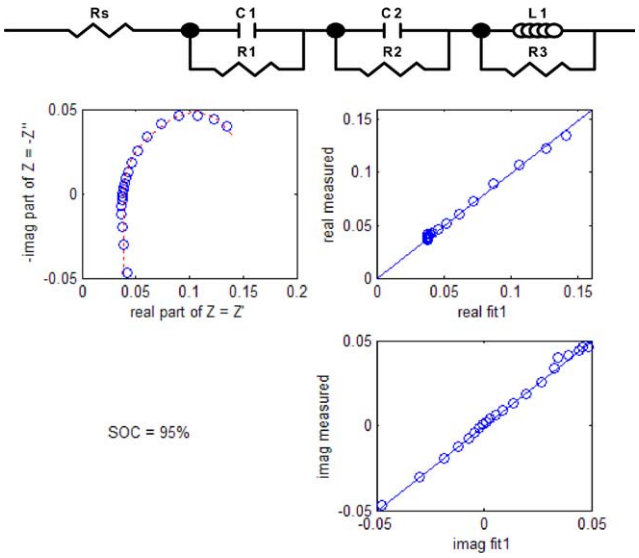

Fig. 4. (Clockwise from top right.) The Nyquist plot of EIS for SOC = 95% Measured and calculated values of real and imaginary parts of impedance using circuit 3a shown on $y = x$ line. Percent relative error = 3.75%.

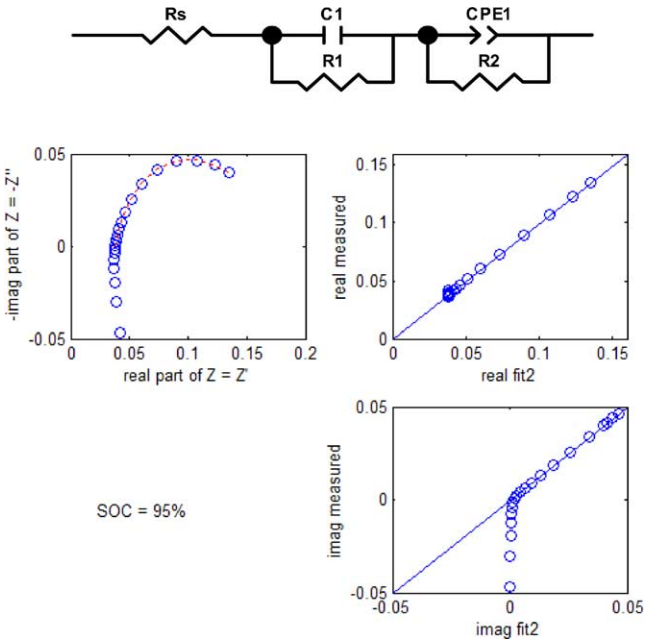

Fig. 5. (Clockwise from top right.) The Nyquist plot of EIS for SOC = 95% Measured and calculated values of real part and imaginary parts of impedance using circuit 3b shown on $y = x$ line. Percent relative error = 19.2%.

of the former. Figs. 8 and 9 likewise show the results for circuits 3b and 2b. Lastly, to underscore the importance of fitting EIS data to a suitable circuit configuration, we show in Fig. 10, the result of applying the sparse algorithm with

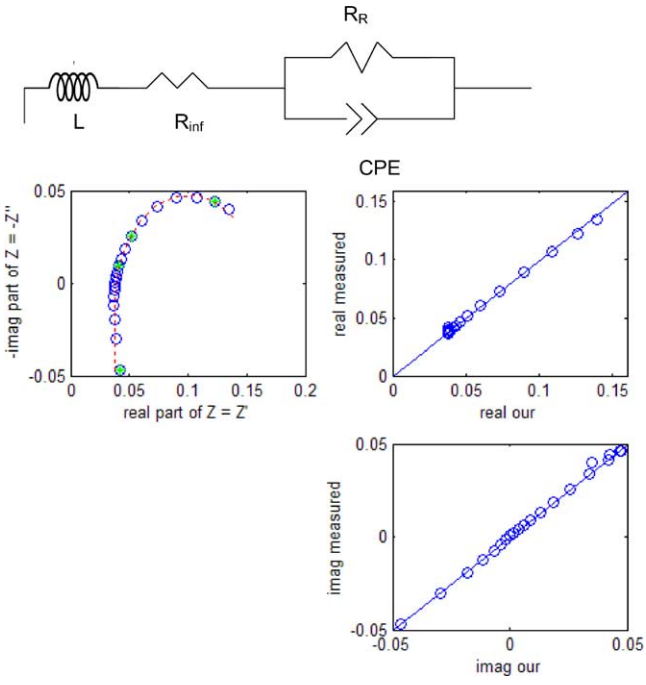

Fig. 6. (Clockwise from top right.) The Nyquist plot of EIS for SOC = 95% Measured and calculated values of real part and imaginary parts of impedance shown on $y = x$ line. Percent relative error = 3.04%. The algorithm selects circuit 2a.

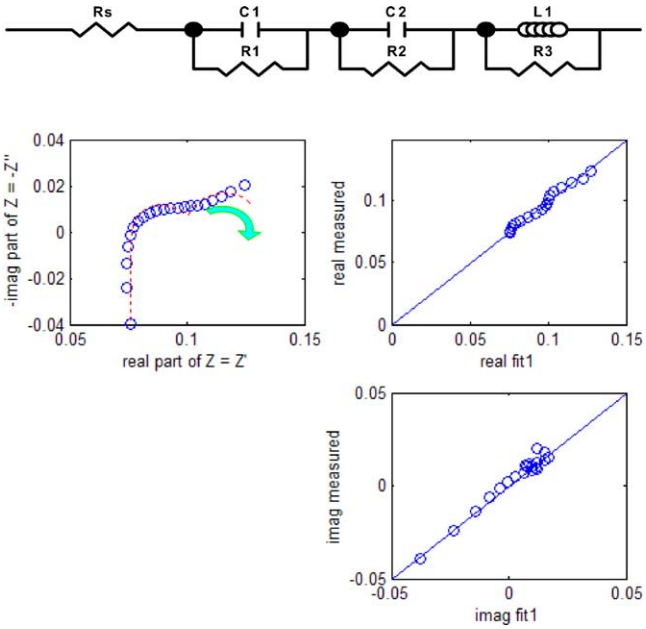

Fig. 7. (Clockwise from top right.) The Nyquist plot of EIS for SOC = 5% Measured and calculated values of real part and imaginary parts of impedance using circuit 3a shown on $y = x$ line. Percent relative error = 3.71%.

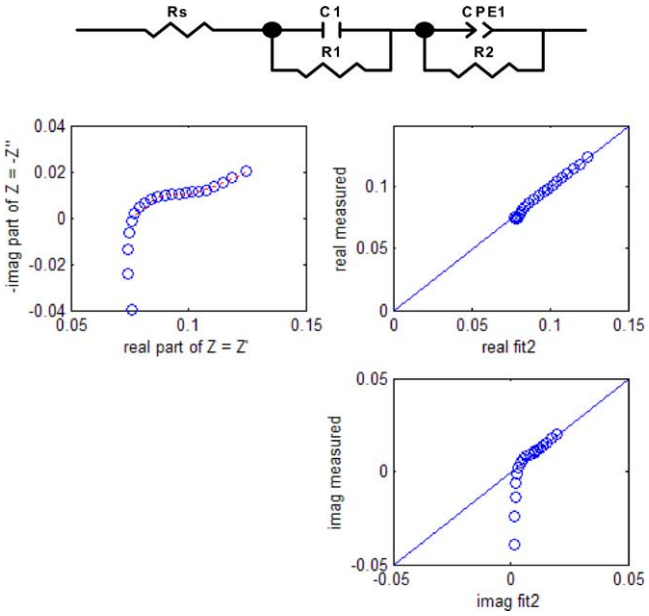

Fig. 8. (Clockwise from top right.) The Nyquist plot of EIS for SOC = 5% Measured and calculated values of real part and imaginary parts of impedance using circuit 3b shown on $y = x$ line. Percent relative error = 12.07%.

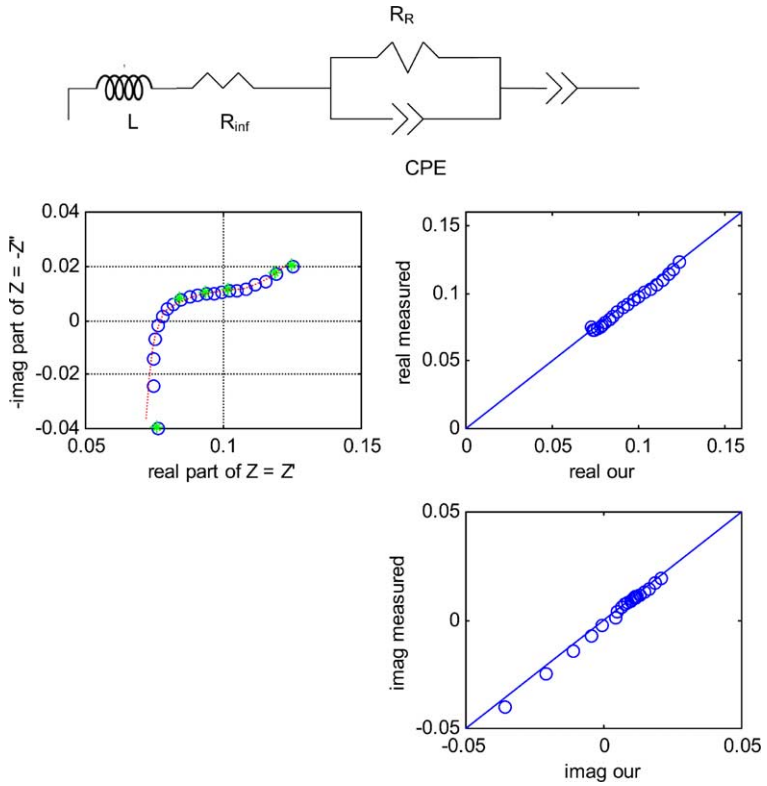

Fig. 9. (Clockwise from top right.) The Nyquist plot of EIS for SOC = 5% Measured and calculated values of real part and imaginary parts of impedance of circuit 2b shown on $y = x$ line. Percent relative error = 2.0083%.

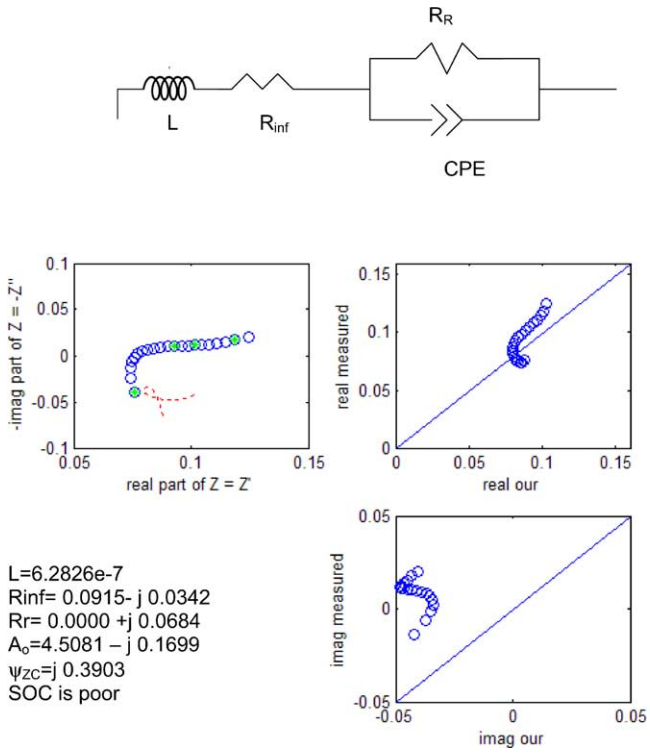

Fig. 10. (Clockwise from top right.) The Nyquist plot of EIS for SOC = 5% Measured and calculated values of real part and imaginary parts of impedance taking circuit 2a shown on $y = x$ line. Percent relativeerror = 52.76%.

three mid-frequency points to the case of 5% SOC. The values obtained are quite anomalous in that complex results are obtained, which is a sure revelation of low SOC because circuit 2a is appropriate for high SOC and a wrong choice for low SOC. The shaded circles in Figs. 6, 9, and 10 show the discrete values used in the sparse algorithm.

5. Conclusion

This paper presents a method for extracting the equivalent circuit parameters of nickel/metal hydride (Ni/MH) batteries, both at low and high SOC using six impedance measurements. When the SOC of a Ni/MH battery is low, EIS curve has a positive slope at the low frequency end suggesting the need for including the Warburg impedance in the equivalent circuit. The proposed method has built into it an SOC-based decision-making capability—both to choose the circuit configuration and to estimate the values of the circuit elements. The impedance back calculated using the estimated circuit parameters is compared with that measured at 21 frequencies. The relative rms %error in the proposed method varied between 2 and 5% whereas using the traditional approach it varied widely in the range 4–25% for different SOC. The circuit topologies chosen are consistent with the physical processes involved in the battery and the computational complexity of the proposed method is less than that of nonlinear least squares technique.

References

[1] C. Witham, A. Hightower, B. Fultz, B.V. Ratnakumar, R.C. Bowman Jr., J. Electrochem. Soc. 144 (1997) 3758.
[2] G. Zheng, B.N. Popov, R.E. White, J. Appl. Electrochem. 28 (1998) 381.
[3] Y. Leng, J. Zhang, S. Cheng, C. Cao, Z. Ye, Electrochim. Acta 43 (1998) 1945.
[4] S. Cheng, J. Zhang, M. Zhao, C. Cao, J. Alloys Compd. 293 (1999) 814.
[5] W. Zhang, M.P. Sridhar Kumar, S. Srinivasan, H.J. Ploehn, J. Electrochem. Soc. 142 (1995) 2935.
[6] N. Cui, J.L. Luo, Electrochim. Acta 45 (2000) 3973.
[7] K.S. Champlin, US Patent 6,037,777 (2000).
[8] S.R. Nelatury, P. Singh, J. Power Sources 112 (2002) 621.
[9] B.A. Boukamp, Solid State Ionics 20 (1986) 31.
[10] J.R. Macdonald (Ed.), Impedance Spectroscopy—Emphasizing Solid Materials and Systems, Wiley, New York, 1987.